# Thermally Reversible Phase Separation in Polystyrene/Poly(styrene-*co*-4-bromostyrene) Blends

**G. R. Strobl,† J. T. Bendler, R. P. Kambour,* and A. R. Shultz**

*Polymer Physics and Engineering Branch, Corporate Research and Development, General Electric Company, Schenectady, New York 12301.* *Received April 1, 1986*

ABSTRACT: Mixtures of a narrow molecular weight distribution polystyrene with poly(styrene-*co*-4-bromostyrene) copolymers obtained by brominating 0.27 and 0.29 mole fraction ($x$) of its units exhibited reversible phase separation at and below their respective upper critical solution temperatures (UCST). An increase of only about 0.02 in $x$ caused an increase of about 70 °C in the UCST of the polystyrene plus poly(styrene-*co*-4-bromostyrene) mixtures. Use of a Nomarski assembly in a polarizing microscope provided excellent contrast for phase detection and structural studies. The liquid–liquid phase boundary (binodal) for mixtures of the $x = 0.27$ copolymer with its parent polystyrene was examined within the framework of Koningsveld's formulation of the Flory–Huggins Gibbs free energy function. A concentration-dependent interaction parameter $g = -0.02949 + (20/T) - 0.007411\phi_2$ provided a good fit of the binodal data above the copolymer volume fraction ($\phi_{2c}$) at the critical point. An interaction parameter $g = -0.00905 + (10/T) - 0.004691\phi_2$ provided a fit that was not as good in the higher $\phi_2$ region but that accommodated the phase boundary data below $\phi_{2c}$ in better fashion. Morphologies of the phase-separated blends varied in a way that was consistent with a nucleation/growth mechanism of separation at the extremes of composition and spinodal decomposition in intermediate ranges. Glass transition temperatures of quenched blends were examined by DSC. One-phase or two-phase character of annealed and quenched blends could be determined thereby, but the small temperature difference in the $T_g$ values (102.5 and 115.6 °C) for the pure blend components made precise detection of incipient phase separation difficult.

## Introduction

High-polymer blend systems suitable for a study of the mechanisms of microphase separation are uncommon. The critical temperature has to lie above the glass transition temperatures of both components and at the same time below the temperature range where rapid chemical decomposition occurs. Until now, only a few systems fulfilling these requirements have been characterized sufficiently to define temperature–composition coexistence curves. McMaster has conducted a structural investigation on blends of poly(methyl methacrylate) and styrene–acrylonitrile copolymers.[1] Nishi, Wang, and Kwei have performed a study on mixtures of polystyrene and poly(vinyl methyl ether).[2] Both systems show LCST behavior with critical temperatures $T_c$ around 140 and 90 °C, respectively. Starting with homogeneous samples, McMaster and Nishi et al., induced phase separation by heating to temperatures above $T_c$. Depending upon the sample composition, structures consistent with a spinodal decomposition mechanism or structures reflecting nucleation and growth were observed. Cloud point curves with LCST's have been also reported by Casper and Morbitzer[3] for polystyrene/poly(tetramethylbisphenol A carbonate), by Roerdink and Challa[4] for poly(vinylidene fluoride)/isotactic poly(ethyl methacrylate), and by Walsh and coworkers[5] for poly(methyl methacrylate)/chlorinated polyethylene. Cloud point curves with UCST's have been reported by Roe and Zin[6] for styrene/butadiene polymer systems of intermediate to high molecular weight. In these systems homogeneous blends at elevated temperatures were cooled to induce phase separation. Recently, Ougizawa, Inoue, and Kammer established a phase boundary including a UCST at about 138 °C for blends of a high molecular weight *cis*-1,4-polybutadiene with a high molecular weight poly(styrene-*co*-butadiene) copolymer.[7] They infer a LCST for the same system from $T$-jump and annealing experiments, producing two-phase mixtures at high temperatures (approximately 200 °C). They report that similar results have been observed for another *cis*-1,4-polybutadiene/poly(styrene-*co*-butadiene) pair and for a poly(acrylonitrile-*co*-styrene)/poly(acrylonitrile-*co*-butadiene) pair.

We have performed a similar study on mixtures of polystyrene with brominated polystyrene. By variation of the degree of polymerization and the level of bromination, compatibility can be controlled[8] and, ultimately, the critical temperature can be continuously shifted. This enables a controlled preparation of blends with critical temperatures in the desired temperature range, 150–300 °C. Phase separation in this system was studied by optical microscopy and calorimetry. As reported in the following, a reversible UCST behavior was found.

## Experimental Section

An anionically polymerized polystyrene, PS2b, with $\bar{M}_n = 2.0 \times 10^4$ and $\bar{M}_w/\bar{M}_n = 1.06$ purchased from Pressure Chemical Co. was chosen as the starting material for copolymer synthesis. Bromination of this resin was effected in a nitrobenzene solution in the dark.[9] Complete bromination was achieved after 22 h of reaction time at 25 °C using 1.2 mol of $Br_2$/mol of styrene units. Lowering this ratio led to partial bromination. Reaction products were precipitated by pouring the solution into rapidly stirred methanol. After filtering they were dried in vacuo at 100 °C until all odor of nitrobenzene had disappeared. The degree of bromination was derived from the $^{13}C$ nuclear magnetic resonance spectrum.

As proved by $^{13}C$ and $^1H$ NMR spectra, bromination occurred exclusively in the 4-position of the aromatic ring, the brominated units being randomly distributed along the chain. Preparation of the statistical styrene–4-bromostyrene copolymer in this manner is particularly advantageous in that the degree of polymerization of the parent polystyrene and that of the derivative copolymer are identical.

Blends of the original polystyrene and the brominated derivative were formed by codissolution in chloroform or methylene chloride followed by film casting or precipitation in methanol. Depending on the bromination level, films were hazy or clear, indicating a two-phase or single-phase structure. For 1:1 mixtures the clarity transition occurred at a molar concentration of brominated units $x \simeq 0.28$. We selected two copolymers with bromination levels close to this critical concentration for the temperature dependent studies: copolymer I with $x = 0.27$; copolymer II with $x = 0.29$.

† On leave from the Institut für Physikalische Chemie, Universität Mainz, Mainz, Federal Republic of Germany; present address: Albert-Ludwigs Universität, Freiburg, Federal Republic of Germany.

0024-9297/86/2219-2683$01.50/0 

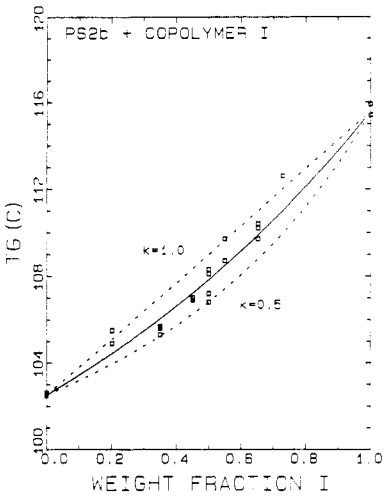


**Figure 1.** Glass transition temperatures of quenched, single-phase polystyrene/copolymer I blends as a function of weight fraction copolymer.

Phase separation and morphology studies were carried out in a polarizing microscope with a Nomarski phase contrast optical assembly. For our samples excellent contrast was provided by this technique. Samples were prepared on a hot stage by squeezing a droplet of the blend between two microslides. Films thus obtained were 10–30 $\mu$m thick. They were inspected at room temperature after a controlled thermal treatment followed by quenching on a metal block.

Calorimetric measurements were performed in a Perkin-Elmer DSC-2C differential scanning calorimeter. Digital data (temperature and differential power) were logged and analyzed by its dedicated microcomputer. All scanning data were taken at 20 °C/min heating rate on 10-mg samples in open or crimp-sealed aluminum cups. Homogeneous blends, annealed at 220 or 230 °C, were quenched effectively by rapid cooling (nominal −320 °C/min) in the calorimeter and gave single glass transitions upon subsequent first heating scans. Two-phase blends were achieved by annealing at temperatures below their binodal temperatures and quenching. The glass transition temperature $T_g$ is defined as the temperature at which the specific heat in the transition region has achieved half the total increase it experiences in transforming from a glass to a nonglass.

## Results

Blends of polystyrene PS2b(1) with copolymer I(2) annealed above 220 °C show a single-phase structure at all compositions. The numerals 1 and 2 are here, and subsequently, used to designate components 1 and 2 in the subject mixtures. Figure 1 presents DSC $T_g$ data for such blends quenched after annealing at 220 or 230 °C. $T_g$ increased smoothly from 102.5 °C for pure polystyrene to 115.6 °C for pure copolymer I as the weight fraction, $w_2$, of the latter was increased. The data were examined within the framework of the Couchman relation:[10]

$$\ln T_g = \frac{\ln T_{g1} + k(w_2/w_1) \ln T_{g2}}{1 + k(w_2/w_1)}$$

The upper, middle, and lower curves shown in Figure 1 correspond to $k$ = 1.0, 0.7, and 0.5, respectively. One notes from Table I that the Couchman relation with $k$ = 0.7 fits the observed average $T_g$ values rather well. The small temperature range (13.1 °C) in $T_g$ between the two pure components makes accurate determination of the best-fit $k$ difficult. However, it does appear to be lower than the ratio, $\Delta C_{p2}/\Delta C_{p1}$ = 0.9, of the measured heat capacity increments at $T_g$ of the polymers ($\Delta C_{p1}$ = 0.29 J g$^{-1}$ deg$^{-1}$; $\Delta C_{p2}$ = 0.26 J g$^{-1}$ deg$^{-1}$).

Annealing of the blends at temperatures in the range 150–220 °C induced phase separation. Two-phase structures visible in the microscope formed within several minutes. The structure change was reversible. Annealing of two-phase structures at 240 °C reproduced the single-phase state. Stirring, i.e., macroscopic shearing of the melt by relative rotation of the microslides, was necessary to achieve the latter transition within reasonable time.

**Table I**
**Approximate Binodal Temperature/Composition Data and Glass Transition Temperature/Composition Data for Polystyrene + Copolymer I Blends**

| | | $T_g$ of quenched blend, °C | |
|---|---|---|---|
| $w_2$ | phase boundary temp, °C | obsd | calcd ($k$ = 0.7) |
| 0.00 | | 102.5 | (102.5) |
| 0.202 | 181 | 105.2 | 104.4 |
| 0.27 | 210 | | |
| 0.349 | 218 | 105.5 | 106.0 |
| 0.45 | 213 | 107.0 | 107.2 |
| 0.50 | 208 | 107.6 | 107.8 |
| 0.55 | 203 | 109.2 | 108.5 |
| 0.652 | 191 | 110.1 | 109.9 |
| 0.73 | 180 | 112.6 | 111.0 |
| 1.00 | | 115.6 | (115.6) |

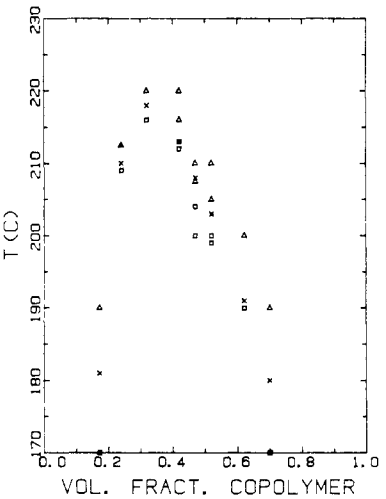


**Figure 2.** Single-phase (△) and two-phase (□) blends of polystyrene/copolymer I in relation to temperature and volume fraction copolymer.

For an approximate determination of the phase boundary (binodal curve), samples of different composition were annealed for a constant time (30 min) at a series of decreasing temperatures on the microscope hot stage. Figure 2 represents the observation, with triangles denoting homogeneous, single-phase melts and squares denoting two-phase melts. The rather large temperature intervals employed in the quench/anneal procedure to provide two-phase melts for subsequent microscopic examination did not allow precise determination of the phase separation temperatures. In estimating the ($\phi_2$, $T$) coordinates of the binodal, we used arithmetic averages of the observed one-phase and two-phase temperatures for the $w_2$ = 0.202, 0.349, 0.55, and 0.73 data. For other compositions, the $T$(binodal) values were weighted toward the more heavily determined (one phase or two phase) observation. This introduces a somewhat subjective, although bounded, estimate of the experimental ($\phi_2$, $T$) coordinates (denoted by × in Figure 2 and presented as ($w_2$, $T$) in Table I). Calculation of theoretical binodal and spinodal curves to approximate the liquid–liquid phase equilibria data is described in the Discussion.

The phase contrast microscopy provided facile detection of phase separation in the blends. DSC could detect with difficulty the phase separation, because the quenched, equilibrated phases differed so little in $T_g$. Inspection of

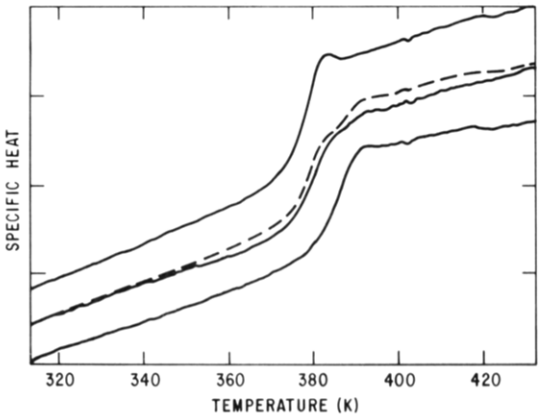


**Figure 3.** DSC curves for single-phase polystyrene/copolymer I blends (upper curve $w_2 = 0.202$; lower curve $w_2 = 0.73$) quenched from 220 °C and a two-phase blend (center curve $w_2 = 0.45$) quenched after 30 min at 180 °C. The broken line represents a 50/50 weight averaging of the upper and lower curves.

Figure 2 shows that annealing at 180 °C a sample having volume fraction copolymer $\phi_2 = 0.42$ ($w_2 = 0.45$) should yield equilibrating phases of nearly equal mass corresponding to the $\phi_2 = 0.18$ ($w_2 = 0.202$) and $\phi_2 = 0.70$ ($w_2 = 0.73$) blends. Figure 3 presents the DSC scans of these latter two blends after quenching from 220 °C and of the $w_2 = 0.45$ blend after annealing for 30 min at 180 °C and then quenching. The broken curve was constructed by weight averaging on a 50/50 weight basis the upper and lower specific heat curves. The correspondence of the observed and calculated curves for the 180 °C annealed blend and the appearance of the glass transition regions for each of the phases are obvious.

To obtain some insight into the character of the phase separation the morphologies of the two-phase systems were examined microscopically.

Figure 4 shows a series of micrographs obtained for blends of the polystyrene with copolymer I with different volume fractions of the brominated component, $\phi_2 = 0.31$, 0.42, 0.47, and 0.62. Phase separations in the originally homogeneous samples were induced by annealing for 2 h at 190 °C. Spherical precipitates in a continuous matrix are observed for $\phi_2 = 0.31$ and 0.62. For $\phi_2 = 0.42$ and 0.47 the phase domains are nonspherical and partly connected.

Figure 5 shows the development of the two-phase structure with time. A sample with $\phi_2 = 0.48$ was annealed at 200 °C. After the first appearance of phase separation followed by an increase in phase contrast, one observes "ripening" of the structure. The coarseness of the interconnected phase domains increases with time.

For samples of the polystyrene blended with copolymer II, the upper critical solution temperature (UCST) was located at about 290 °C. Samples annealed at 300 °C were homogeneous while those annealed at temperatures below 280 °C exhibited phase separation. Since thermal decomposition could not be ruled out at these rather high temperatures,[11] most of our study was confined to blends containing copolymer I. However, we show in Figures 6 and 7 two special examples of phase-separated structures in a polystyrene/copolymer II blend ($\phi_2 = 0.48$). The micrograph Figure 6 was obtained after 30 min of annealing at 200 °C. The domains of both phases are strongly interconnected. Figure 7 shows the macroscopic phase domains developed after 2 h of annealing at 250 °C.

## Discussion

The general character of the observed reversible transition between single-phase and two-phase states is clear;

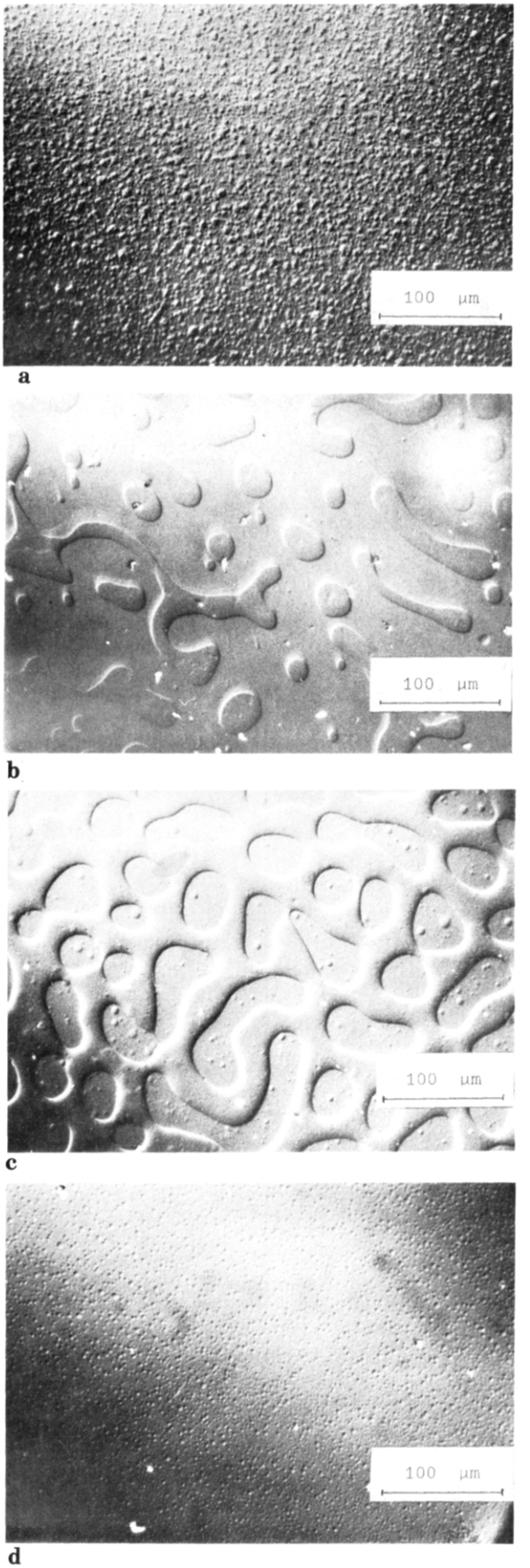


**Figure 4.** Two-phase structures of polystyrene/copolymer I blends induced by annealing for 2 h at 190 °C. Volume fractions of the copolymer: (a) 0.31; (b) 0.42; (c) 0.47; (d) 0.62.

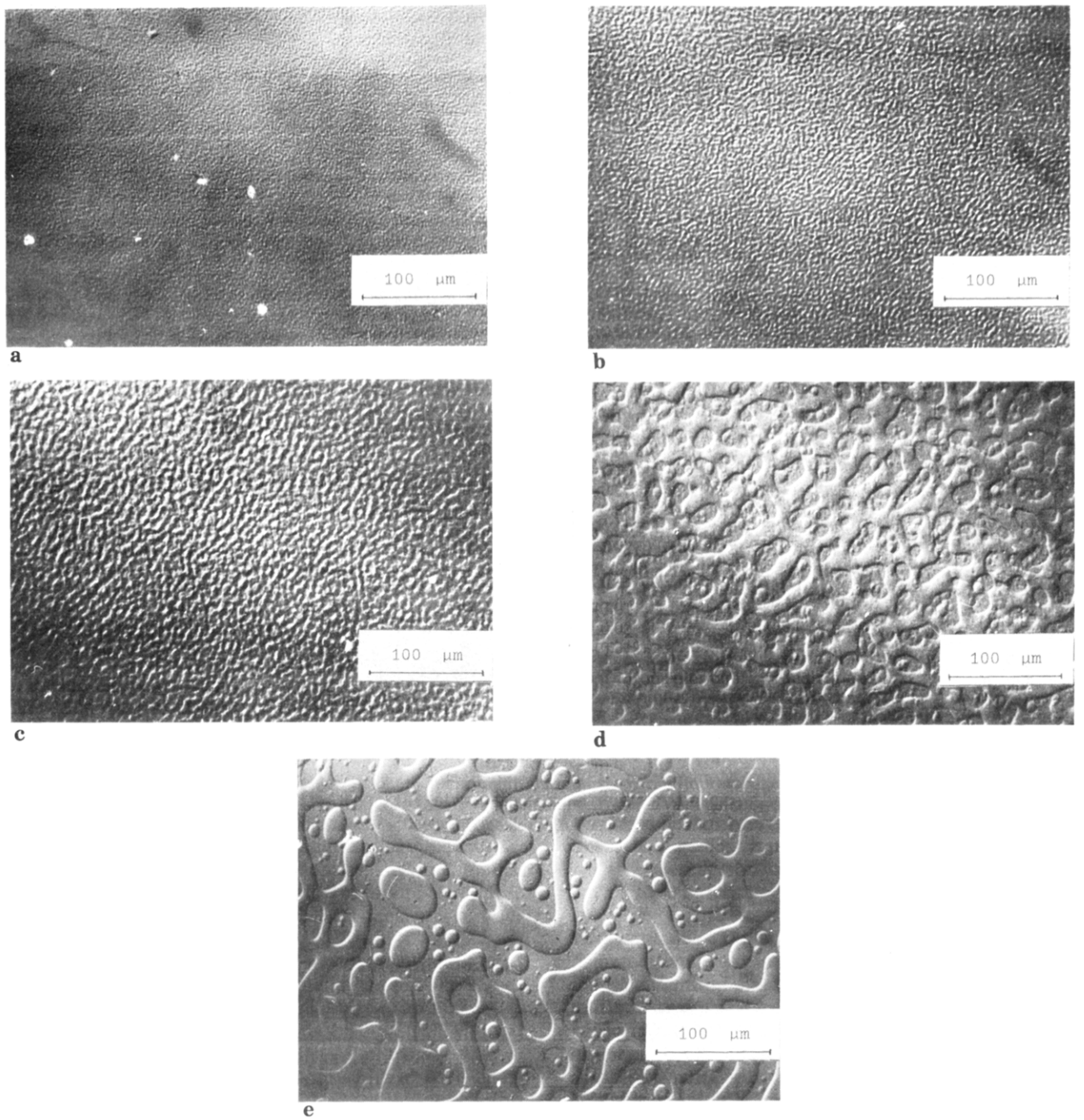


**Figure 5.** Structure development during phase separation in a polystyrene/copolymer I blend ($\phi_2 = 0.48$). Micrographs were obtained during annealing at 200 °C for (a) 1, (b) 3, (c) 10, (d) 30, and (e) 90 min.

the investigated blends exhibit an upper critical solution temperature. Direct evidence is provided by the appearance of the miscibility gap shown in Figure 2.

The occurrence of a UCST in our system can be understood on the basis of existing theories.[12] Miscibility depends upon the balance between the favorable combinatorial entropy of mixing

$$-T\Delta S_c = RT\left(\frac{\phi_1}{N}\ln\phi_1 + \frac{\phi_2}{N}\ln\phi_2\right) \qquad (1)$$

where $N$ denotes the degree of polymerization, and the change in local free enthalpy

$$\Delta G_{loc} = RT\chi\phi_1\phi_2 \qquad (2)$$

which is here expressed in terms of the Flory–Huggins interaction parameter $\chi$ per unit.

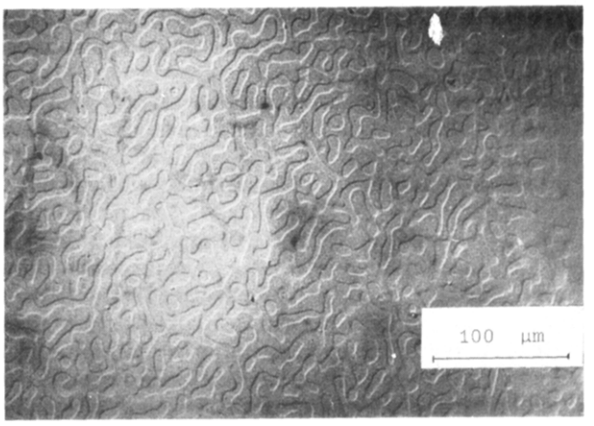


**Figure 6.** Interconnected domains in the two-phase structure of a polystyrene/copolymer II blend ($\phi_2 = 0.48$) after 30 min at 200 °C.

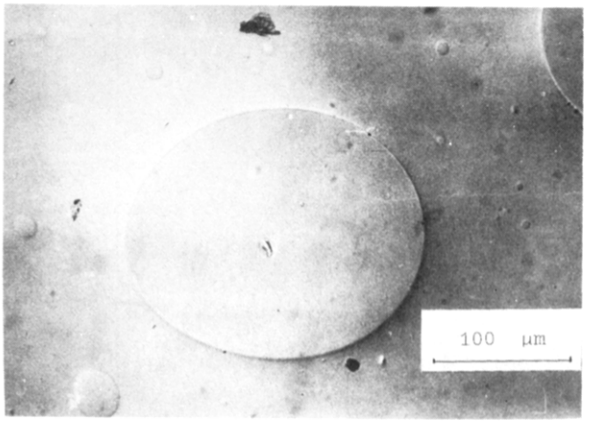


**Figure 7.** Macroscopic domains in a two-phase polystyrene/copolymer II blend ($\phi_2 = 0.48$) after 2 h at 250 °C.

Assuming $\chi$ is not a function of $\phi_2$, its value at the critical temperature is

$$\chi(T_c) = 2/N \tag{3}$$

in both cases, UCST or LCST.

Given the temperature dependence of $\chi$, eq 3 determines the critical temperatures of a blend.

According to Patterson[13] the $\chi$ parameter includes two contributions

$$\chi(T) = \frac{-U(T)}{RT}\frac{X_{12}}{P^*} + \frac{C_p(T)}{2R}\tau_{12}^2 \tag{4}$$

the first one being associated with the contact-energy dissimilarity and the second one following from the difference in thermal expansion between the two components. The difference in contact energy is specified by the dimensionless quantity $X_{12}/P^*$, the difference in thermal expansion by the quantity $\tau_{12}$. The temperature dependence of $\chi$ enters via the cohesive energy $-U(T)$ and the specific heat $C_p(T)$, which can be taken for either component or the blend (the differences are unimportant in this approximation).

In the system under study, $X_{12}/P^*$ and $\tau_{12}$ depend on the bromination level $x$. Specifically, a short calculation given in the Appendix shows that

$$X_{12} = x^2 X_{AB} \tag{5}$$

$$\tau_{12} = x\tau_{AB} \tag{6}$$

where $X_{AB}$ and $\tau_{AB}$ specify the contact energy and thermal expansion differences between polystyrene and poly(4-bromostyrene). Introduction of eq 5 and 6 into eq 4 gives

$$\chi(T) = x^2\chi_{AB}(T) \tag{7}$$

Combination of eq 7 and 3 then leads to

$$2/Nx^2 = \chi_{AB}(T_c) \tag{8}$$

Equation 8 describes the variation of critical temperatures with the bromination level and the molecular weight. Figure 8 illustrates in a schematic drawing the situation. Assuming that $X_{AB} > 0$, $\chi_{AB}(T)$ first decreases, goes through a minimum, and then increases again. At low temperatures the contact energy term dominates; at high temperatures the expansion term becomes more important. If $2/Nx^2$ takes on a value as indicated in the drawing, two critical temperatures, one UCST and one LCST, show up. Increasing the bromination level or the degree of polymerization raises the UCST and lowers the LCST, finally leading to a coalescence and disappearance. Note that only the product $Nx^2$ enters into eq 8. Hence, an increase in $N$ could be compensated by a decrease in $x^2$, leaving the phase behavior of the blend unchanged.

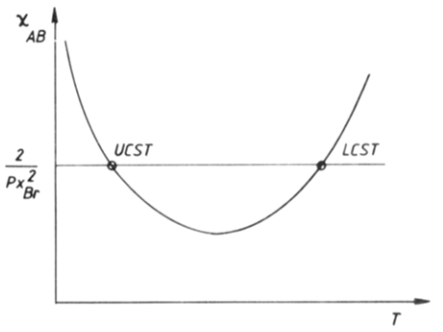


**Figure 8.** Temperature dependence of the interaction parameter $\chi_{AB}$ (schematic drawing).

For the current system this analysis indicates that the temperature at the minimum of $\chi_{AB}(T)$ lies above 300 °C, i.e., outside the temperature range accessible for experiments. Therefore, one can only observe the UCST branch of the phase diagram.

The above discussion tacitly assumes a composition-independent $\chi_{AB}$ and equal molar volumes for the polystyrene and the copolymer obtained from its partial bromination. To treat the polystyrene (1)–copolymer I (2) blend phase equilibria in a more quantitative fashion, we here resort to the thermodynamic formulation by Konigsveld[14] of the Flory–Huggins Gibbs free energy.

The Gibbs free energy of mixing per mole of lattice sites is expressed by

$$\Delta G = RT\left[\frac{(1-\phi_2)\ln(1-\phi_2)}{N} + \frac{r\phi_2\ln\phi_2}{N} + g\phi_2(1-\phi_2)\right] \tag{9}$$

A styrene chain unit is chosen as the lattice site definition. $N$ is the number of chain units in the polystyrene molecule. $r$ is the ratio of the molar volume of the parent polystyrene to the molar volume of the copolymer. $\phi_2$ is the volume fraction (site fraction) of the mixture occupied by the copolymer.

A composition-dependent interaction parameter is here employed:

$$g = g_0(T) + g_1\phi_2 \tag{10}$$

$$g_0(T) = W + Y^*(T^{-1} - T_c^{-1}) \tag{11}$$

where $T_c$ is the critical temperature for phase separation and $W$ and $Y$ are constants.

Partial differentiation of eq 9 with respect to the moles of the constituent polymers yields the chemical potentials.

$$\mu_1 - \mu_1^\circ = RT[\ln(1-\phi_2) + (1-r)\phi_2 + Ng_0\phi_2^2 + Ng_1(2\phi_2 - 1)\phi_2^2] \tag{12}$$

$$\mu_2 - \mu_2^\circ = RT[\ln\phi_2 + (1-r^{-1})\times (1-\phi_2) + Ng_0r^{-1}(1-\phi_2)^2 + 2Ng_1r^{-1}\phi_2(1-\phi_2)^2] \tag{13}$$

The second and third partial derivatives of the Gibbs free energy with respect to $\phi_2$ are

$$\partial^2\Delta G/\partial\phi_2^2 = RT\left[\frac{r}{N\phi_2} + \frac{1}{N(1-\phi_2)} + 2(g_1 - g_0) - 6g_1\phi_2\right] \tag{14}$$

$$\partial^3\Delta G/\partial\phi_2^3 = RT\left[\frac{r}{N\phi_2^2} + \frac{1}{N(1-\phi_2)^2} - 6g_1\right] \tag{15}$$

At the critical temperature ($T_c$) and critical composition ($\phi_{2c}$) for phase separation the expressions in eq 14 and 15

are simultaneously zero. Therefore, from eq 15 one obtains

$$g_1 = \frac{1}{6N}\left[ -\frac{r}{\phi_{2c}^2} + \frac{1}{(1-\phi_{2c})^2} \right] \quad (16)$$

and from eq 14 and 16

$$g_0 = \frac{1}{2N}\left[ \frac{r}{\phi_{2c}} + \frac{1}{1-\phi_{2c}} \right] + g_1(1 - 3\phi_{2c}) \quad (17)$$

The number of units per chain in the polystyrene and copolymer I is $N = 20000/104.15 = 192$. An approximate ratio, $r = V_1/V_2$, of the polymer molar volumes is obtained by using bulk (glass) specific volumes of 0.943 and 0.637 for styrene and *p*-bromostyrene homopolymers, respectively, and assuming volume additivity of units in the $x = 0.27$ copolymer I. This yields $r = 0.952$. Calculation of theoretical binodal and spinodal curves to compare with the approximate binodal $T,\phi_2$ data (Table I) was done as follows.

Using $\phi_{2c} = 0.30$ and $T_c = 491$, one calculates by eq 16 and 17 that $g_1 = -0.007411$ and $g_0(491\ \text{K}) = 0.01124$. Then $g = 0.01124 + Y(T^{-1} - 491^{-1}) - 0.007411\phi_2$. For temperatures $T < 491$ K the chemical potential functions (eq 12 and 13) exhibit a maximum and minimum value within a range of $\phi_2$ values. The value of $Y = 20$ was found to give a good fit for the $\phi_2 > \phi_{2c}$ binodal data points when $\phi_2,\phi_2'$ pairs satisfying the simultaneous $\mu_1 - \mu_1^\circ = \mu_1' - \mu_1^\circ$ and $\mu_2 - \mu_2^\circ = \mu_2' - \mu_2^\circ$ conditions were determined. The calculated binodal and the calculated spinodal (eq 14 set equal to zero) are shown in Figure 9a with the experimental binodal data points. Inspection of Figure 9a reveals an excellent fit of the $\phi_2 > \phi_{2c}$ binodal data using the pair interaction parameters

$$g = -0.02949 + (20/T) - 0.007411\phi_2 \quad (18)$$

or the equivalent Flory pair interaction parameter reduced to the pair interaction parameter per styrene unit

$$\chi/N = g_0 - g_1 + 2g_1\phi_2 = -0.02208 + (20/T) - 0.01482\phi_2 \quad (19)$$

Despite the excellent fit of the calculated binodal to the data in the higher $\phi_2$ region, the calculated binodal lies well above the two $\phi_2 < \phi_{2c}$ experimental points.

Using $\phi_{2c} = 0.35$ and $T_c = 491$ K, we found by the procedure just described that $g = 0.01132 + 10(T^{-1} - 491^{-1}) - 0.004691\phi_2$ produced a binodal passing through the experimental $(\phi_2, T) = (0.24, 483\ \text{K})$ point and intersecting the experimental $\phi_2 > \phi_{2c}$ binodal at about $(\phi_2, T) = (0.56, 471\ \text{K})$. The calculated binodal and spinodal are shown in Figure 9b with the experimental binodal data points. Forcing the binodal to fit the experimental $(\phi_2, T) = (0.24, 483\ \text{K})$ data point yields (cf. Figure 9b) a poorer match of the calculated binodal to the data for $\phi_2 > \phi_{2c}$. However, the anomaly of having the experimental binodal data points in the $\phi_2 < \phi_{2c}$ region lie below the calculated spinodal has been removed. We are compelled to conclude that the lack of precision in delineating the binodal by the present data makes determination of the interaction parameter subject to considerable uncertainty. Therefore, although the UCST character and approximate shape of the liquid–liquid phase boundary have been reproduced by the above approach using the Flory–Huggins Gibbs free energy formulation, a quantitative, unique solution was not achieved.

The morphologies of the phase-separated melts as revealed by the optical microscopic examinations permit postulation of the modes of phase separation. The observed structures (Figures 4–7) indicate that two different

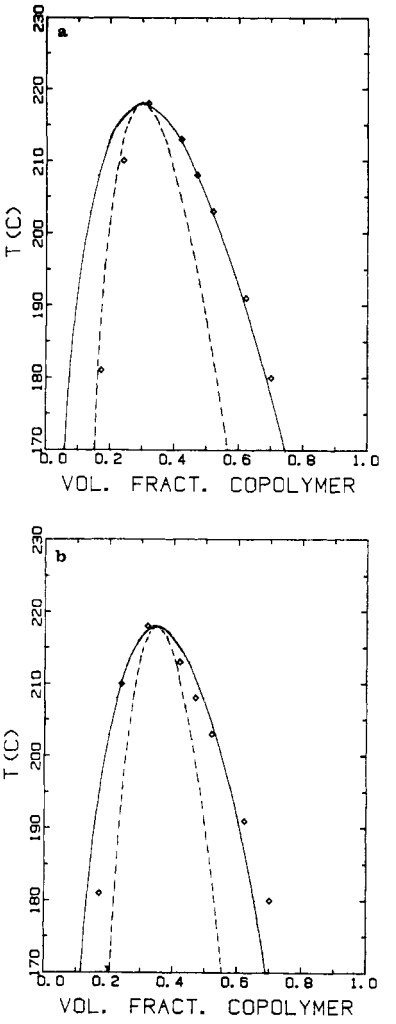


**Figure 9.** (a) Binodal (solid curve) and spinodal (broken curve) calculated by using $\phi_{2c} = 0.30$ and $T_c = 491$ K. The diamonds represent experimental points on the phase boundary. (b) Binodal (solid curve) and spinodal (broken curve) calculated by using $\phi_{2c} = 0.35$ and $T_c = 491$ K. The diamonds represent experimental points on the phase boundary.

mechanisms of phase separation are operating in different regions of composition. The spherical droplets dispersed in a continuous matrix, as in Figure 4a,d, are consistent with the nucleation and growth mechanism expected to operate in the region between the binodal and spinodal. The continuous structures (particularly that in Figure 6 wherein both phases are interconnected and indistinguishable in shape) suggest spinodal decomposition into the equilibrating phases. Thus, blend compositions far removed from the critical composition favor binodal (nucleation and growth) phase separation while blend compositions near the critical composition favor spinodal (spontaneous) phase separation.

**Acknowledgment.** This research was performed during the residency of G.R.S. as a Visiting Research Fellow at the General Electric Corporate Research and Development Center in the Summer of 1981. We acknowledge the assistance of Mrs. A. L. Young in the calorimetric studies.

## Appendix

The exchange interaction parameter $X_{12}$, which specifies the difference in contact energies between polymers 1 and 2, was introduced by Flory[15] as

$$X_{12} = \frac{s}{2v^*}(\epsilon_{11} + \epsilon_{22} - 2\epsilon_{12})$$

The $\epsilon$ parameters describe the contact energies between the respective pairs of segments. In the case of copolymer mixtures each $\epsilon_{ij}$ has to be understood as the mean contact energy between the copolymers $i$ and $j$ (the other parameters, $s$ and $v^*$, denote the coordination number and the hard-core segment volume, respectively).

In the case of interest, mixtures of polystyrene (segments A) and copolymers with a fraction $x$ of brominated segments (B), the $\epsilon$ parameters become

$$\epsilon_{11} = \epsilon_{AA}$$

$$\epsilon_{22} = x^2\epsilon_{BB} + 2x(1-x)\epsilon_{AB} + (1-x)^2\epsilon_{AA}$$

$$\epsilon_{12} = (1-x)\epsilon_{AA} + x\epsilon_{AB}$$

where $\epsilon_{AA}$, $\epsilon_{AB}$, and $\epsilon_{BB}$ denote the contact energies between styrene–styrene, styrene–bromostyrene, and bromostyrene–bromostyrene segment pairs. Insertion of these expressions results in

$$X_{12} = \frac{s}{2v^*}x^2(\epsilon_{AA} + \epsilon_{BB} - 2\epsilon_{AB})$$

or

$$X_{12} = x^2X_{AB}$$

with

$$X_{AB} = \frac{s}{2v^*}(\epsilon_{AA} + \epsilon_{BB} - 2\epsilon_{AB})$$

The second parameter, $\tau_{12}$, appearing in eq 4 has been introduced by Patterson[13] to specify the dissimilarity in thermal expansion, that is, in free volume between the two polymeric components. It is defined as

$$\tau_{12} = 1 - T_1^*/T_2^*$$

where $T_1^*$ and $T_2^*$ denote the reduction temperatures of the two components to be used with the scaled equation of state. Assuming

$$T_2^* - T_1^* \approx x(T_B^* - T_A^*)$$

where $T_A^*$ and $T_B^*$ denote the reduction temperatures of polystyrene and polybromostyrene, gives

$$\tau_{12} \approx x\tau_{AB}$$

with

$$\tau_{AB} = 1 - T_A^*/T_B^*$$

**Registry No.** PS, 9003-53-6.

## References and Notes


(1) McMaster, L. P. *Polym. Prepr. (Am. Chem. Soc., Div. Polym. Chem.)* **1974**, *15*, 254.
(2) Nishi, T.; Wang, T. T.; Kwei, T. K. *Macromolecules* **1975**, *8*, 227.
(3) Casper, R.; Morbitzer, L. *Angew. Makromol. Chem.* **1977**, *58/59*, 1.
(4) Roerdink, E.; Challa, G. *Polymer* **1980**, *21*, 1161.
(5) Walsh, D. J.; Higgins, J. S.; Zhikuan, C. *Polymer* **1982**, *23*, 336.
(6) Ougizawa, T.; Inoue, T.; Kammer, H. W. *Macromolecules* **1985**, *18*, 2089.
(7) Roe, R. J.; Zin, W.-C. *Macromolecules* **1980**, *13*, 1221.
(8) Kambour, R. P.; Bendler, J. T. *Macromolecules*, preceding paper in this issue.
(9) Kambour, R. P.; Bendler, J. T.; Bopp, R. C. *Macromolecules* **1983**, *16*, 753.
(10) Couchman, P. R. *Macromolecules* **1978**, *11*, 1156.
(11) Malhotra, S. L.; Lessard, P.; Blanchard, L. *J. Macromol. Sci., Chem.* **1981**, *15*, 279.
(12) Paul, D. R.; Newman, S., Eds. *Polymer Blends*; Academic: New York, 1978; Vol. 1, Chapters 1–3.
(13) Patterson, D.; Robard, A. *Macromolecules* **1978**, *11*, 690.
(14) Koningsveld, R. Ph.D. Thesis, University of Leiden, 1961.
(15) Flory, P. J. *Discuss. Faraday Soc.* **1970**, *49*, 7.


# Separation and Characterization of Cyclic Sulfides Formed in the Polycondensation of Dibromoalkanes with Aliphatic Dithiols


**G. Montaudo,*† C. Puglisi,‡ E. Scamporrino,† and D. Vitalini‡**

*Dipartimento di Scienze Chimiche, Università di Catania, 95125 Catania, Italy, and Istituto per la Chimica e la Tecnologia dei Materiali Polimerici, Consiglio Nazionale delle Ricerche, 95125 Catania, Italy.*

*Received March 6, 1986*


ABSTRACT: Mass spectrometric and gel permeation chromatographic analyses are used to identify the cyclic oligomers formed in the polycondensation reactions of dithiols and dibromoalkanes leading to aliphatic polysulfides. A correlation exists between the two sets of data obtained by these techniques. Cyclic oligomers with only an even number of repeating units are detected among the polycondensation reaction products. This fact is considered evidence that these oligomers are generated directly from the reacting monomers and not by degradation of the corresponding polymers.


## Introduction

The formation of cyclic oligomers in polycondensation reactions is a phenomenon frequently observed.[1-3]

Current methods of detecting oligomers contained in polymer samples are based on gas, liquid, and size exclusion chromatography, combined with some structural identification methods. These techniques are indeed powerful, but sometimes low volatility of samples, low solubility in suitable organic solvents, or low resolution in liquid chromatography make alternative and rapid methods of detection and identification of complex mixtures of low molecular weight compounds highly desirable.

Mass spectrometry (MS) is particularly suitable for the detection of these materials since they are volatile under high vacuum at relatively mild temperatures at which polymers remain undecomposed and therefore undetected.[4-6]

We have been interested in the synthesis and characterization of a series of polysulfides: $-((CH_2)_6S)_n-$, poly(hexamethylene sulfide) (I); $-((CH_2)_3S)_n-$, poly(trimethylene sulfide) (II); $-((CH_2)_2S)_n-$, poly(ethylene sulfide) (III); and $-(CH_2S)_n-$, poly(methylene sulfide) (IV). These


† Università di Catania.
‡ Istituto per la Chimica e la Tecnologia dei Materiali Polimerici.


0024-9297/86/2219-2689$01.50/0 